Available online at www.sciencedirect.com

SciVerse ScienceDirect

Energy Procedia 37 (2013) 4628 – 4634

Energy Procedia

GHGT-11

Development of carbon dioxide microbubble sequestration into saline aquifer and CO_2-EOR reservoirs

Ziqiu Xue [a,*], Shinya Tsuji [b], Hiromichi Kameyama [c], Susumu Nishio [c], Toshifumi Matsuoka [b]

[a] *Research Institute of Innovative Technology for the Earth (RITE), 9-2 Kizugawadai, Kizugawa, Kyoto, 619-0292, Japan*
[b] *Dept. of Civil and Earth Resources Engineering, Kyoto University, Kyotodaigaku-Katsura, Nishikyo-ku, Kyoto, 615-8510, Japan,*
[C] *Tokyo Gas Co., Ltd, 1-7-7 Suehiro-Cho Tsurumi-Ku, Yokohama, 230-0045, Japan*

Abstract

CO_2 microbubble injection into saline aquifers can accelerate CO_2 dissolution and trapping and minimize the free CO_2 in the subsurface. As CO_2 is dissolved in formation water, it will change the pH and CO_2 will be converted into stable carbonate minerals as a result of geochemical reactions. These trapping mechanism contribute effectively to the long term safety of large-scale CO_2 storage. CO_2 microbubble sequestration is also a novel technology to store CO_2 from the small- to middle-scale emission sources such as oil refinery and hydrogen filling station, by enhanced dissolution and effective use of pore space suggested by our experimental results.

Selection and/or peer-review under responsibility of GHGT

Keywords: CO_2 microbubble; enhanced dissolution; geophysical monitoring; P-wave velocity; resistivity

1. Introduction

CO_2 microbubble injection has been proposed as an option to inject CO_2 from the small- to middle-scale emission sources into widely existing monoclinic reservoirs in Japan [1, 2]. Injection CO_2 in microbubble can be achieved by installing special porous filters on borehole casing or gas tubing [3]. Xue et al. [2] successfully generated microbubble CO_2 in gaseous, liquid and supercritical phases by using special porous filters. Compared to other methods such as shock wave and shear flow, special porous filter has advantages in installation and cost. They also showed the enhanced effect for dissolution of CO_2

* Corresponding author. Tel.: +81-774-75-2312; fax: +81-774-75-2313.
E-mail address: xue@rite.or.jp.

1876-6102
Selection and/or peer-review under responsibility of GHGT
doi:10.1016/j.egypro.2013.06.371

microbubble. From the quantitative analysis with images recorded by a high-speed digital video camera system, they concluded that the enhanced effect of microbubble was higher than 20%.

The first dataset of CO_2 dissolution into formation water was collected at the Japanese Nagaoka pilot CO_2 injection site [4]. Figure 1 shows the low resistivity zone (marked in blue) around the free-CO_2-beraing zone (marked in red) detected by time-lapse well logging. This result suggests the CO_2 dissolution significantly increased the ion concentration in formation water and recently the formation water sampling result shows the potential carbonate mineral precipitation [5].

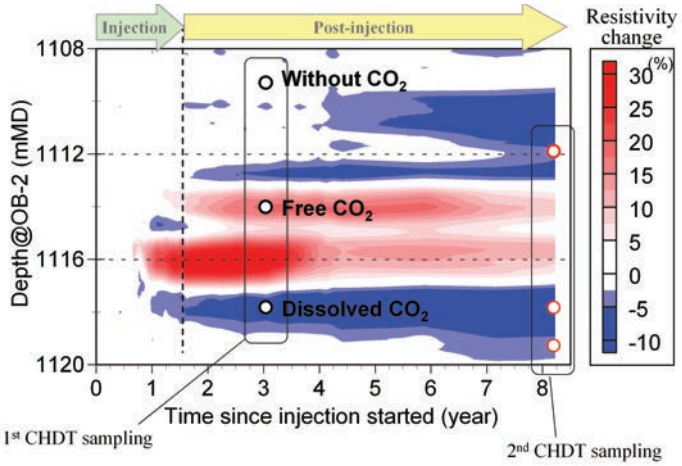

Fig. 1. CO_2 distribution within a high permeable layer in the reservoir from the time-lapse resistivity well logging results at observation well OB-2 at Nagaoka site. The blue and red colors indicate changes in resistivity (Mito and Xue).

The time scale of carbonate mineralization process at the Nagaoka site is much shorter than the anticipated one in the IPCC special report [6]. One of the reasons is the low salinity of formation water. The low salinity will increase the solubility of CO_2 in formation water and then will reduce the pH and cause geochemical reactions in early stage. Consequently such processes effectively contribute to the safety of CO_2 storage. These enhanced processes will take place in the same manner as we inject CO_2 microbubble into saline aquifer and oil reservoirs.

To improve understanding of enhanced processes in CO_2 microbubble sequestration, we carried two CO_2 injection experiments with same porous sandstone and measured P-wave velocity and resistivity changes when injecting CO_2 in microbubble with a grooved disc with small holes (Case A) and injecting CO_2 through a special porous filter (Case B). We compared the differences in P-wave velocity and resistivity changes between Case A and Case B and discussed the advantages in CO_2 microbubble injection and geophysical monitoring in CO_2 microbubble sequestration.

To assist interpretation of P-wave and resistivity results in Cases A and B, we used X-ray CT to visualize CO_2 migration in pore spaces by injecting CO_2 into the same sandstone sample through the special porous filter and the grooved disc with small holes. In this paper we present the advantages of CO_2 microbubble in both saline aquifer storage and enhanced oil recovery from low-production and depleted oil reservoirs.

2. Experimental Procedure

2.1. P-wave velocity and resistivity measurements

Two cylindrical Berea sandstone samples (50 mm in diameter and 100 mm in length, 18% porosity) were used in laboratory measurements of P-wave and resistivity in two case studies. Figure 1 shows the configurations of the piezoelectric transducers and the electrodes. Two electrodes shaped into a 50 mm diameter cylinder were attached at the top and bottom of the sample, and four ring electric potential electrodes with a 2.5 mm width strip were attached on the sample surface. The electrodes were silver coated copper mesh coated with silver in order to avoid corrosion in low pH fluids. The piezoelectric transducers have a characteristic frequency of 1 MHz. Sixteen piezoelectric transducers were cemented to the sample covering almost whole area of the lateral section of the sample when the injected CO_2 migrating from bottom toward to top side of the sample. A grooved disc with small holes was set to the bottom side in Case A and a special porous filter was used in Case B to generate CO_2 microbubble.

The whole sample assembly was covered by silicon sealant to prevent the leakage of CO_2 from the sample and invasion of hydrostatic pressure medium (oil) into the sample. After setting the sample into the pressure vessel, it was pressurized up to 13MPa under hydrostatic pressure conditions. Then the sample was saturated with artificial formation water (0.01Mole, KCL solution, 1 ohm-m) in 10MPa. Supercritical CO_2 was injected into the water-saturated sandstone at 10.5MPa, 40 ºC and 0.05ml/min. The hydrostatic pressure and pore pressure were kept constant throughout the CO_2 injection test.

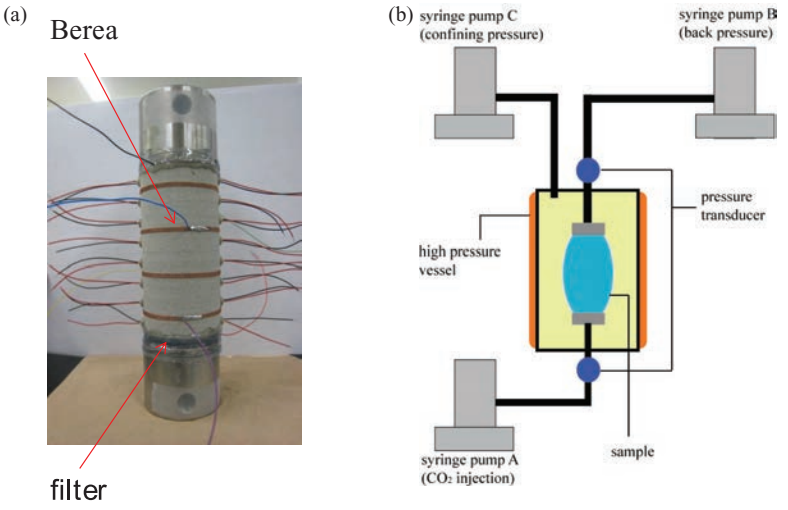

Fig. 1. (a) Berea sandstone with piezoelectric transducers and electrodes;
(b) Schematic diagram of wave velocity and resistivity experiment system.

2.2. X-CT Visualization of CO_2 Migration in pore spaces

X-ray computed tomography (X-CT) is a powerful tool for visualizing the injected CO_2 in pore structure of porous sandstones. In this study we used the Toshiba Aquilion One X-CT Scanner with a resolution of 0.35mm x 0.35mm, to monitor and evaluate changes in the fluid saturations in Berea sandstone (35mm in diameter and 70mm in length). Figure 2 shows the sample prepared for the X-CT

visualization test. The grooved disc was set to left end and the special filter was set to right end of the sample. The assembled sample was set into a special pressure vessel designed for X-CT scanner. The pressure and temperature conditions were set as same as the experiments of P-wave velocity and resistivity measurements. CO_2 was injected first through the grooved disc from the left end of the sample and then the sample was flushed with artificial formation water to remove CO_2 in pore spaces until the CT value recovered to the initial saturated condition. Then CO_2 was injected through the special filter from right end of the sample. X-CT images were recorded during the two injection tests, to investigate advantages of CO_2 microbubble injection.

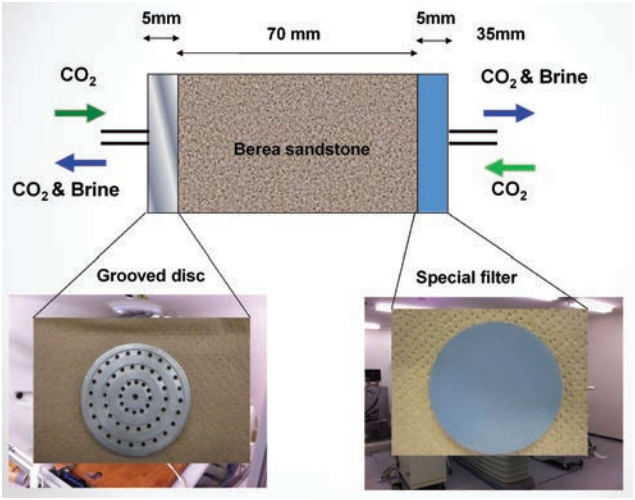

Fig. 2. Schematic view of the sample assembly for X-CT visualization test. The grooved disc and special filter were set to the left and right ends respectively to simulate CO_2 injections in Case A and Case B in wave velocity and resistivity measurements.

3. Results and Discussion

3.1. Results of the P-wave velocity and resistivity experiments

P-wave velocity will decrease and resistivity will increase as a result of CO_2 and water displacement in pore spaces in water-saturated sandstones. Usually changes in P-wave velocity and resistivity depend on CO_2 flooding sweep efficiency. Higher sweep efficiency causes large changes in P-wave velocity and resistivity. Figure 3 shows the P-wave velocity changes obtained from experiments Case A and Case B. P-wave velocity begins to decrease when the CO_2 front across the ray path. Therefore Figure 3 shows how the injected CO_2 migrating from the bottom end toward the top end of the sample. It took about 120 minutes for CO_2 to reach the bottom end of the sample, due to the dead volume of pore water in pore pressure line.

Breakthrough time of injected CO_2 in Case A is about 280 minutes and it is almost double the breakthrough time in Case B. CO_2 injected through the grooved disc migrated at a steady pace in Case A and this result suggests once a flow path formed, the path will dominate the CO_2 flow in this sample. If the CO_2 does not penetrate into other pore spaces, the sweep efficiency would be low and ultimately cause an early breakthrough of injected CO_2.

In Case B CO_2 was injected through a special filter and the CO_2 behavior is quite different from that in Case A. Besides the breakthrough time, the time interval between two ray paths becomes longer from the bottom to the top end. P-wave velocity reduction in Case A is littler lager than that in Case B. It is worth to point out that the reduction rate becomes smaller from bottom to the top end in Case A. But in Case B the large reduction of P-wave velocity appeared at the upper part of the sample.

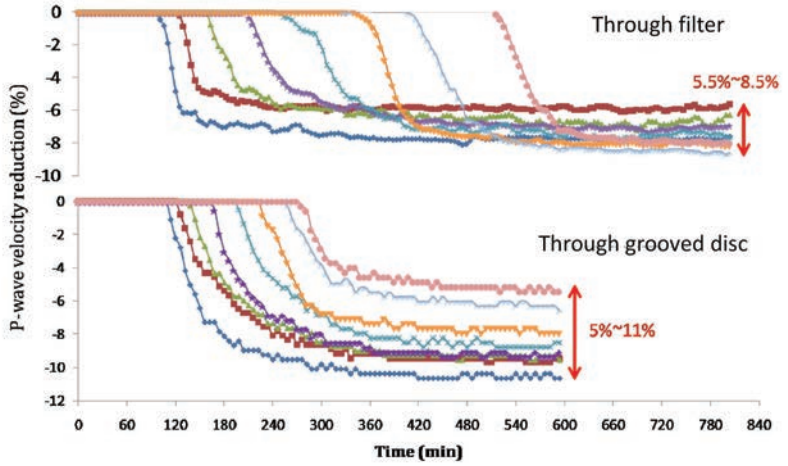

Fig. 3. P-wave velocity reduction vs elapsed time in Case A (lower) and Case B (upper). In Case A CO_2 was injected through the grooved disc and in Case B CO_2 was injected through the special filter to generate CO_2 microbubble.

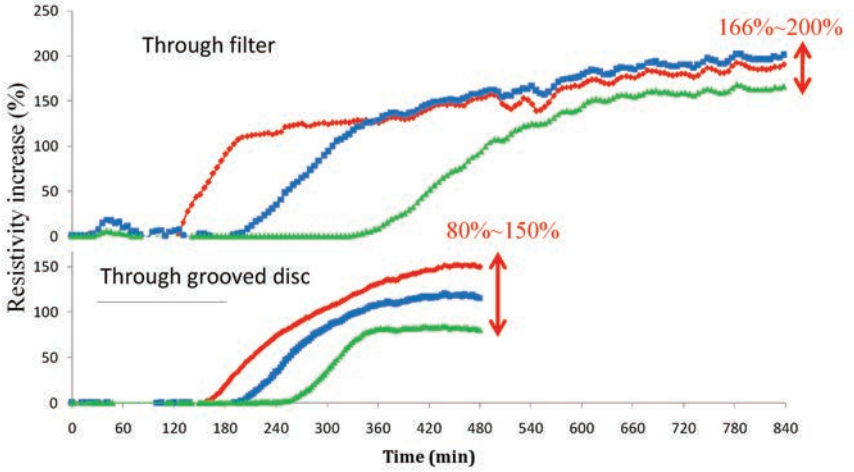

Fig. 4. Resistivity increase vs elapsed time in Case A (lower) and Case B (upper).

Figure 4 shows resistivity changes obtained from the CO_2 injection tests of Case A and Case B. Usually resistivity will decrease as CO_2 dissolution into pore water. In this study resistivity was measured between two ring electric potential electrodes. In Figure 4 resistivity measured at the lower, middle and

upper part of the sample was shown in Red, Yellow and Green color, respectively. Resistivity increase in lower part in Case B is earlier than that in Case A and the time gap becomes small at the middle part. It is interesting that in Case B resistivity increase at the upper part is later than in Case A and the resistivity increase for each part in Case B is larger than that in Case A. These results suggest that CO_2 injection through the special filter leads to better sweep efficiency in CO_2 microbubble flooding.

3.2. Results of the X-CT visualization of CO_2 distribution in pore spaces

In this study we used X-CT scanner to monitor the injected CO_2 behavior and to evaluate the CO_2 saturation throughout the sample. By comparing the results obtained from CO_2 injection through the special filter and the grooved disc. Figure 5 shows the CO_2 distribution changes in a cross section during CO_2 injection.

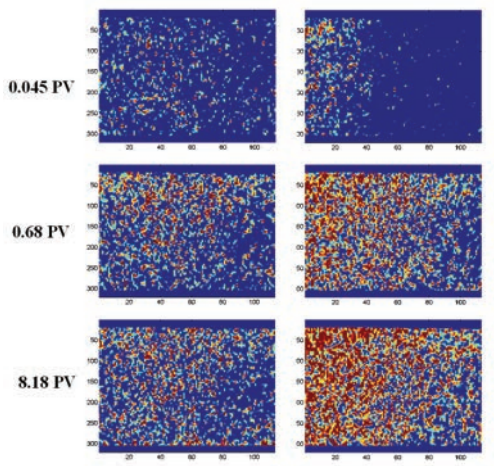

Fig. 5. CO_2 distribution (left: grooved disc; right: special filter) in a cross section of Berea sandstone. The numbers indicate volume of injected CO_2 into the sample.

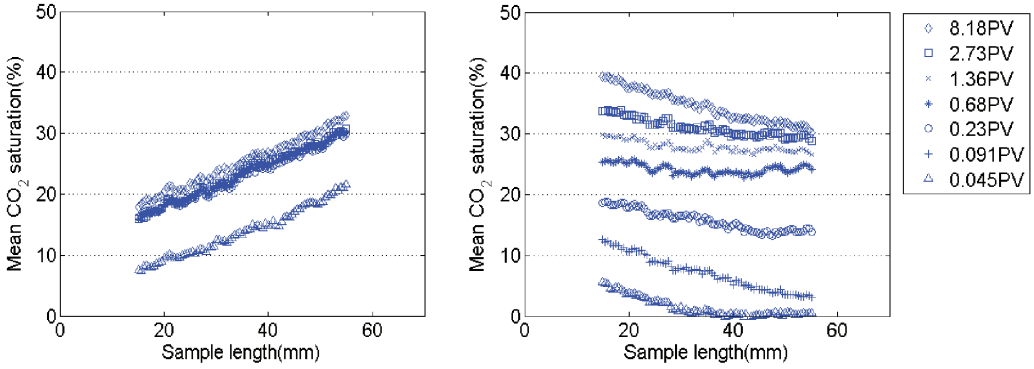

Fig. 6. Changes of mean CO_2 saturation (left: grooved disc; right: special filter) along the sample length during CO_2 injection.

Figure 6 shows the mean CO_2 saturation changes along the sample length during injection of CO_2 into the sample. When injecting CO_2 through the grooved disc the CO_2 distribution showed a little change even the CO_2 volume increased from 0.68 PV (Pore Volume) to 8.18 PV. This result agreed well with the CO_2 saturation change along the sample length. In Figure 6 beyond 0.091 PV the mean CO_2 saturation is almost constant and this result suggests that the flow path for CO_2 formed and in this case the sweep efficiency is low. When injecting CO_2 through the special filter the migration of CO_2 front is slow and this leads the late CO_2 breakthrough. The late breakthrough depends on CO_2 dissolution and effective use of pore spaces. The CO_2 microbubble dissolution can be clearly confirmed in cases of 0.045 PV and 0.091 PV in Figure 6. In case of 0.045 PV the injected CO_2 completely dissolved into pore water when the CO_2 front reached just half of the sample length. During the CO_2 microbubble injection the CO_2 saturations in Figures 5 and 6 increased significantly around the injection end of the sample. These results suggest the usefulness of CO_2 microbubble injection in enhanced oil recovery.

4. Conclusions

We examined the CO_2 microbubble injection into saline aquifers can accelerate CO_2 dissolution and trapping and minimize the free CO_2 in the subsurface. From the X-CT visualization experiments we clearly confirmed the CO_2 microbubble dissolution in pore water. The practical use of this technology is to install the special filter directly to the gas tubing or steel casing in injection wells. Based on the Nagaoka field survey results we could conclude that CO_2 microbubble injection will accelerate CO_2 dissolved in formation water and CO_2 will be converted into stable carbonate minerals as a result of geochemical reactions. These trapping mechanism also contribute effectively to the long term safety of large-scale CO_2 storage. In the near future CO_2 microbubble sequestration would be a novel technology to store CO_2 from the small- to middle-scale emission sources such as oil refinery and hydrogen filling station. CO_2 microbubble injection shows the advantages in the effective use of pore space and our experimental results suggest that higher sweep efficiency of CO_2 microbubble injection will contribute to the enhanced oil recovery from the low permeable and depleted reservoirs.

References

[1] Koide H, Xue Z., Carbon microbubble sequestration: a novel technology for stable undergrand emplacement of greenhouse gases into wide variety of saline aquifers, fractured rocks and tight reservoirs, Energy Procedia 2009, 3655-3662.

[2] Xue Z., Yamada T., Matsuoka T., Kameyama H. and Nishio Susumu, Carbon dioxide microbubble injection — Enhanced dissolution in geological sequestration; Energy Procedia 2011, 4307-4313.

[3] PCT: WO 2010/018844 A1, Storing device for stored substance and method for storing stored substance.

[4] Mito S. Xue Z. and Ohsumi T., Case study of geochemical reactions at the Nagaoka CO_2 injection site, Japan. *Int J Greenhouse Gas Control*, 2008; 2: 309-318.

[5] Mito S and Xue Z, Geochemical trapping of CO_2 in saline aquifer storage:Results of repeated formation fluid sampling at the Nagaoka site, the 11th International Conference of Greenhouse Gas Control Technilogies, 2012, Kyoto Japan.

[6] IPCC, 2005. Special Report on Carbon Dioxide Capture and Storage, Cambridge University Press: New York.